Identification of constitutive laws' parameters by means of experimental tests on AlSi-PE abradable coating

B. Chevrier, J. Vincent, L. Faure, Sylvain Philippon

Identification of constitutive laws' parameters by means of experimental tests on AlSi-PE abradable coating

B. Chevrier[a,b], J. Vincent[a], L. Faure[a], S. Philippon[a]

[a] *Université de Lorraine, CNRS, ENIM, LEM3, F-57000 Metz, France*
[b] *Safran Aircraft Engines, Réau, Rond-Point René Ravaud, 77551 Moissy-Cramayel, France*

Abstract

Abradable coatings are a part of dynamic seals used in aircraft engines to diminish inter-stage leakages by reducing rotor/stator clearances of the low and high-pressure compressors. However, interactions may occur during running between the rotating blades and the coating sprayed onto the casing. Due to the complexity of reproducing experimentally rotor/stator interactions, modeling approaches are used to optimize the choice of abradable coating, making constitutive laws necessary input data for rotor/stator interaction studies. Previous experimental researches were done to explore the dynamic and quasi-static compressive thermomechanical behavior of AlSi-PE abradable coating [1, 2]. Using results from these investigations and from a complementary experimental characterization coupled with a high speed camera, parameters of a standard Johnson-Cook constitutive law have been identified for the wide ranges of strain-rate and temperature explored. Although modeling data were in satisfactory agreement with the experimental results, an original constitutive law formulation has been proposed to better predict the thermomechanical behavior of AlSi-PE abradable material at high temperatures. As an introduction of damage into the modeling, a standard and modified Johnson-Cook damage law, describing a strain criterion from which failure theoretically begins, has been included and analyzed when modeling the coating's behavior by considering only quasi-static conditions.

Keywords : abradable, coating, AlSi-PE, thermomechanical behavior, DIC, constitutive law, damage law, Johnson-Cook

1. Introduction

The main purpose of aircraft engines manufacturers is to optimize the global efficiency of their turbomachines. One solution is to reduce functional clearances between the rotor and the stator for limiting inter-stage leakages in the compressor and turbine stages [3]. Reducing these clearances increases the probability of creating undesirable contact between the high-speed rotating blades and the casing. To prevent rotating parts of getting damaged during interaction, abradable coatings are introduced as sacrificial layer

thermally sprayed onto the inner casing surface. The heterogeneous and porous nature of these coating, made up of different phases of materials, must be both easily removable by the blade to limit its wear and resistant to the erosion due to air flows. Abradable coatings are mostly used in LPCs (Low Pressure Compressors) or in HPCs (High Pressure Compressors), where severe conditions take place, such as high strain-rates or high temperatures [4].

In order to understand abradable coatings behavior under these conditions, many test rigs have been developed over the last decades. Experimental benches recreating specific interactions between simplified blades and abradable coatings [5–10] or full-scale investigations [11, 12] were designed and used for this purpose. The results led to a better understanding of wear mechanisms taking into account the conditions of interactions such as relative velocity, blade incursion rate or temperature [4–9]. Borel et al. [4] and Schmid [13] used the Sulzer Innotec incursion test facility in order to characterize wear of AlSi-PE abradable coating in extreme conditions, for example with coating temperatures ranging from room temperature up to 1200 °C or with blade tip velocity ranging from 100 m/s up to 500 m/s. Through the built wear maps of both research works, AlSi-PE coating can be clearly identified as sensitive to blade tip velocity and wear that occurs during rubbing. Within the framework of severe interactions between a fixed simplified Ti6Al4V blade tip and a moving AlSi-PE coating specimen led on the LEM3's test rig, Martinet et al. [14] also underlined a mechanical behavior dependent on temperature through the expression of a specific force criterion in regard to the following test temperatures : room temperature, 125 °C, 175 °C and 270 °C.

Hence, it seems that numerical simulations are a good way to characterize abradable seal systems. Efforts taken in this direction by engines manufacturers [15] and researchers [16] demonstrate a real interest in this approach. Nonetheless, this strategy requires a good understanding of how the whole set of materials used in conditions representative of aircraft engine contexts express their thermomechanical behavior. Legrand et al. [17] proposed a numerical simulation strategy which consists in modeling abradable coating wear profiles in representative conditions after a defined number of blade rounds. Abradable coating wear profiles are determined by the unidirectional compressive solicitation of the coating, discretized into the succession of one-directional bar elements, imposed by the blade rotational movement (reduced to one super element). The compressive behavior of coating numerical elements is governed by a bilinear elastoplastic constitutive law. Based on this strategy, Batailly et al. [18] first improved the bilinear constitutive law to account for coating viscosity. As a second step, their study aimed to calibrate the bilinear law's parameters by confronting them with experimental interaction configurations conducted on the LEM3's test facility (fixed tool and moving AlSi-PE specimen). However, due to the fact that numerous aspects have to be accounted for in the experimental results analyses, the identified law parameters values did not physically reflect the mechanical behavior of the AlSi-PE abradable coating. Skiba et al. [1] met a need for material characteriza-

tion by proposing a thermoelastoviscoplastic bilinear constitutive law based on dedicated thermomechanical quasi-static and dynamic experimental investigations on cylindrical AlSi-PE specimens. Although the identified law's parameters values were consistent from a qualitative point of view, the constitutive law failed to accurately capture the abradable material behavior at high temperatures from a quantitative point of view. Pellegrino et al. [19] also characterized quasi-static and dynamic behavior of Metco 601 coating through engineering stress and strain data. Their results exhibited a noticeable strain-rate dependence at room temperature and at 100 °C in comparison with results at 300 °C. However, their work did not approach the topic of constitutive laws formulation and the experimental investigations were conducted on a limited range of strain-rates.

By considering these results taken from literature and from previous research work, using well-known constitutive laws with a formalism that corresponds to experimental observations seemed very interesting. Therefore, the first objective was to correlate results from previous experimental campaigns [1, 2] with a Johnson-Cook (JC) constitutive law. This choice was mainly motivated by its frequent implementation in common finite element method software and its phenomenological basis. For correlation purposes, experimental results must be expressed as true values, which can be done if two main assumptions are verified, i.e. a homogeneous deformation of the specimen and the conservation of its volume during loading, both of which are generally considered as true for metallic materials. By taking into account the particular nature of abradable coatings, these assumptions have been confirmed through the coupling of a SHPB test conducted on an AlSi-PE cylindrical specimen at room temperature, with a high speed camera using an image processing method. Given the outcomes of the JC constitutive law application, an original formulation named ASPECL (AlSi-PE Constitutive Law) has been proposed to account for the specific AlSi-PE thermoviscoplastic behavior. Thanks to these results, the specific behavior of AlSi-PE coating became easier to forecast, especially at high temperatures. Finally, the last step of this article consists in the introduction of a modified JC damage law coupled with the ASPECL formulation with a view to predicting theoretical strain to failure of AlSi-PE coating throughout strain evolution. This investigation has only been carried out under quasi-static conditions for the tests leading to failure and within a certain range of temperatures.

2. Experimental overview

2.1. Materials and sample preparation

The AlSi-PE abradable coating studied here is mainly made up of an aluminum-silicon metallic matrix PAC901 (88 % Al; 12 % Si) sprayed with polyester. This abradable coating is used in the LPC, operating at temperatures up to 360 °C, being the high temperature limit imposed by the melting temperature of the polymer [16]. The description of the AlSi-PE abradable material and the sample preparation method are detailed in the previous article [1].

2.2. Experimental techniques

All the experiments presented in this study, and in the previous article regarding the thermomechanical behavior of AlSi-PE abradable at high strain-rates [1], have been conducted through the Split Hopkinson Bar (SHB) technique. This technique allows for greater precision in characterizing a specimen at high strain-rates (ranging from 10^2 to 10^4 s^{-1}) under a compressive [17, 20], tensile [21] or torsional [22] solicitation. Since this study must be representative of a radial blade tip incursion into the abradable coating, the major part of the tests depicted in this article were done using the Split Hopkinson Pressure Bar (SHPB) technique. Considering AlSi-PE abradable material is sprayed in the LPC of aircraft engines, where temperature can rise up to 360 °C, a heating device enabling a reach of temperature up to 800 °C was used for these investigations. Furthermore, thanks to a robotic arm with a clamping system, the abradable specimen was quickly shifted from the tubular furnace to the axis of compression. SHPB tests proposed by Skiba et al. [1] were conducted using a striker, incident bar and transmitted bars in Inconel 718. This choice can be explained by a satisfactory incident/reflected waves ratio due to an acceptable mechanical impedance matching between AlSi-PE specimen and Inconel 718 bars. In addition, a pulse shaping technique was used in order to impose a nearly constant strain-rate and to contribute to a better equilibrium state of the specimen during its loading [23]. Pulse shapers were Ø15 mm cylindrical samples made of brass and located between the striker and the incident bar. With the Inconel 718 bars setup, the diameter of the bars/strikers was 20 mm, and the bars and the strikers were 2000 mm long and 600 mm long respectively. The elastic waves propagation theory and the SHPB apparatus principle were detailed in the previous study [1]. Additionally, quasi-static tests were performed using an *Instron 5585H* testing machine. AlSi-polyester coating was submitted to an uniaxial compression at 0.0017 s^{-1} at room temperature, 150 °C, 250 °C, 300 °C and 350 °C [2].

3. Results & discussion

3.1. Deformation behavior of AlSi-PE abradable coating

In the experiments of Skiba et al. [2] regarding the thermoelastoviscoplastic modeling the AlSi-PE abradable behavior through a bilinear compressive law, strains and stresses obtained through experimental tests were given as engineering values. In order to correlate SHPB test results on AlSi-PE abradable specimens with Johnson-Cook constitutive and damage laws, strain and stress must be expressed as true values. True strain ε_T and true stress σ_T can be calculated from engineering ones ε_{Eng} and σ_{Eng} using the following relations :

$$\varepsilon_T = \ln(1 + \varepsilon_{Eng}) \tag{1}$$

$$\sigma_T = \sigma_{Eng}(1 + \varepsilon_{Eng}) \tag{2}$$

For this purpose, tested specimens have to be representative of the abradable's macroscopic behavior. Considering equation 2, specimens must conserve their volume and deform homogeneously throughout the first loading of the bars. All the conditions mentioned above have been investigated in this study in order to consider using modeling laws such as Johnson-Cook's. To ensure that the behavior observed during experimental tests corresponds to the macroscopic behavior of the abradable coating, a previous analysis regarding the Representative Elementary Volume (REV) was carried out by Skiba et al. [2]. Results showed that, at a stable normalized porosity level, an REV has been identified for a cubic volume approximated at 0.1 mm^3. Thus a cubic volume with a characteristic length of 0.5 mm corresponds to the identified REV. To account for the three different specimen sizes [2], this estimated REV ensures a macroscopic response of the AlSi-PE coating material.

As mentioned previously, conservation of the volume is necessary and deformation of the specimen during its first loading must be evenly distributed to express results with true values. For this unique purpose, dedicated high speed camera experiments (*Shimadzu HPV2*) with a 312 x 260 pixels resolution have been conducted at a frame rate of 500 kfps on a Ø10 mm AlSi-PE specimen with a speckle pattern for Digital Image Correlation (DIC) purposes. The first objective was to quantify volume variation through geometric measurements of the specimen. The evolution of the specimen thickness can be calculated from its initial thickness and the displacements of the bars through the signals of the strain gauges for the duration of the test.

Based on an image processing method, the diameter of the sample can be measured from images recorded by means of the high speed camera using a Matlab® script. Specimen measurements during dynamic tests can be carried out thanks to other experimental methods. For instance, Ramesh and Narasimhan [24] used a laser occlusive radius detector that measured the diameter of the sample through an entire SHPB test. In our particular case, the choice to conduct this experiment with an image processing method was mainly motivated by the fact that a high speed camera was at our disposal.

Figure 1 shows the procedure used in this study to quantify the diameter evolution during the loading period. The red zone indicates all the pixel columns where the image processing diameter measurements were done. For each pixel line, the mean gray level, noted $\overline{GL}$, was computed to reduce the effect of the speckle pattern and discontinuous contrast (as the specimen top edge magnification shows). As illustrated, the mean gray level expression in function of the pixel lines can be described as a trapezoidal shape with a rising edge, a plateau and a falling edge. The slopes of the rising and falling edges are mainly due to the variation in brightness caused by the cylindrical shape of the specimen. In order to find the top/bottom limits of the specimen on each frame, both the starting point of the rising edge and the ending point of the falling

edge need to be precisely determined. The rising and falling edges were estimated by both intersections (red crosses) between two linear functions (in blue) with the pixel line axis, which defines the limits of the specimen and measures the specimen diameter in pixels, which can further be converted to millimeters.

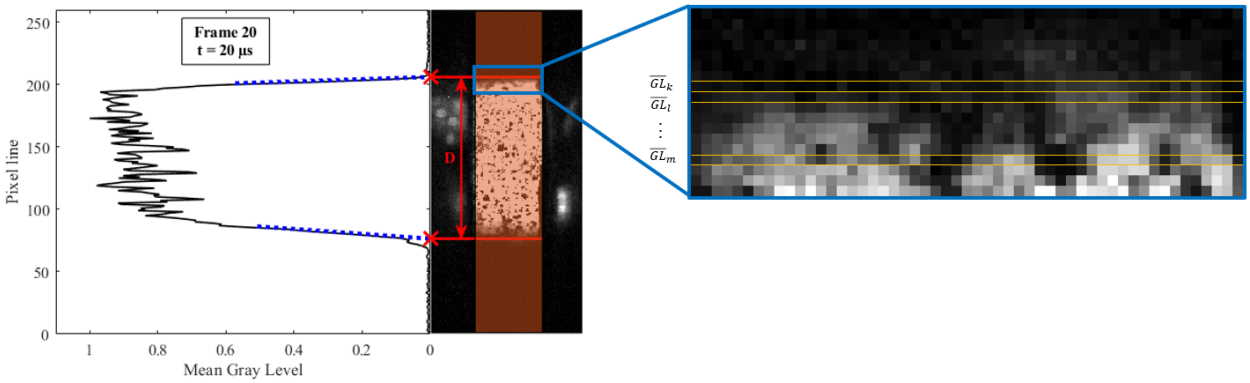

Figure 1: Measurement of the specimen diameter through a high speed photography experiment

Assuming a two-pixel error on the diameter and negligible error on the thickness measurement, the volume calculation uncertainty is close to ±3%. The results obtained from the volume measurement for the loading duration are presented on Figure 2. The maximal volume variation during the high strain-rate compression test of an AlSi-PE specimen has been estimated at 6%. This slight volume decrease during loading could come from any elastic deformation and/or densification of the specimen. Nevertheless, this estimation underlined a satisfactory volume conservation of the AlSi-PE abradable coating.

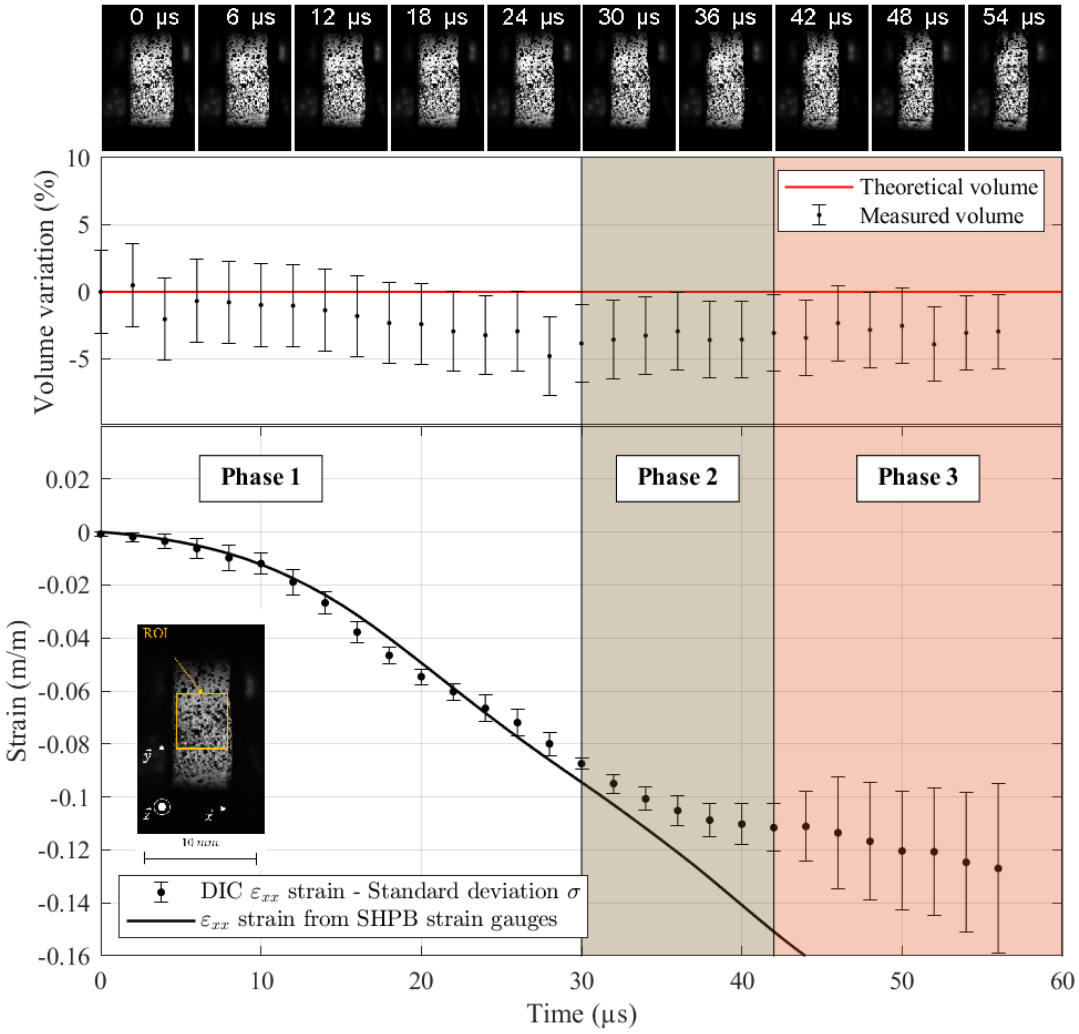

Figure 2: Volume variation and ε_{xx} mean strain estimation obtained by DIC method for a dedicated test on a Ø10 mm AlSi-PE specimen

To determine whether the strain field of the sample is homogeneous, DIC (Digital Image Correlation) calculations were also conducted using the *Ncorr* open-source software [25] running on Matlab®. Results can be seen in Figure 2. ε_{xx} strain (along the loading axis) has been analyzed through a speckle pattern (at a frame rate of 500 kfps). As mentioned previously, the middle area was clearer and brighter than both extremities considering the cylindrical shape of the specimen. Consequently, a square ROI (Region Of Interest) approximately placed in the middle of the specimen has been chosen to conduct optimal displacements analyses. Through the defined ROI, the homogeneity of the strain field is expressed according to the standard deviation of the ε_{xx} strain mean value calculated for each frame during the loading period.

All calculations were made by neglecting radial displacements (off plane) along the z axis. As shown in Figure 2, the results highlighted that the loading period can be divided into three main phases. In the first phase, standard deviation is relatively constant with a maximal measurement dispersion of 6% and ε_{xx} strain measured by SHPB strain gauges matching DIC ε_{xx} strain. The second phase is defined by a mismatch between SHPB and DIC data. This phenomenon could be explained by potential internal damage occurring in the specimen and which cannot be detected with the DIC calculation method. This assumption cannot be validated by post-mortem analysis of the specimen due to its multiple loads induced by the SHPB technique. It must be emphasized that DIC calculations over the third phase do not represent any physical phenomenon. Nevertheless, phase 3 exhibits a much greater standard deviation caused by visual fractures across the specimen.

As a result, despite the porous and heterogeneous nature of AlSi-PE abradable, the experimental analysis depicted in this section tends to point out to a homogeneous deformation during the first loading period (phase 1). Thus, SHPB results from thermomechanical characterization can be expressed according to true strain and true stress values. The correlation between these experimental results and Johnson-Cook modeling is now relevant.

3.2. Thermomechanical behavior of AlSi-PE abradable coating

During dynamic compression of a sample, adiabatic heating takes place due to plastic strain energy being transformed into heat. Therefore, the temperature of the sample is varies during its solicitation. This variation can be expressed with equation 3.

$$\Delta T = \frac{Q}{mC_p} \tag{3}$$

where ΔT represents the temperature rise (K), Q the heat energy (J), m the mass of the sample (kg) and C_p the specific heat capacity (J.kg^{-1}.K^{-1}). In order to estimate heat, Taylor and Quinney [26] proposed a β coefficient which is used to quantify the percentage of plastic strain energy W converted into heat Q. This particular coefficient is generally set at 90% for metallic materials. Rittel et al. [27] showed that for dynamic loading this coefficient depends on the material nature, the loading mode and the strain-rate within the sample. For two different aluminum alloys, the Taylor-Quinney coefficient has been estimated between 20% and 40%. Even if AlSi-PE is mainly made of aluminium, the heterogeneous and anisotropic nature of it prevents any Taylor-Quinney coefficient estimation in this range. Thereby a 90% β coefficient was used for this adiabatic heating estimation, knowing that it may overestimate the temperature rise during compression. The expression of the temperature rise in function of true stress σ_T and true plastic strain $\varepsilon_{P,T}$ can be seen in equation 4. The true plastic strain $\varepsilon_{P,T}$ is defined in equation 5, where E corresponds

to the Young modulus of the studied material.

$$\Delta T = \frac{0.9W}{mC_p} = \frac{0.9 \int \sigma_T d\varepsilon_{P,T}}{mC_p} \tag{4}$$

$$\varepsilon_{P,T} = \varepsilon_T - \frac{\sigma_T}{E} \tag{5}$$

Other authors, such as McLellan and Ishikawa [28], exhibited an aluminium's Young modulus linear dependence to temperature. From this assumption, Skiba et al. [2] carried out cyclic quasi-static compression tests on a 20 mm diameter and 10 mm thickness AlSi-PE specimen at a strain-rate of 0.0017 s^{-1} using a standard testing machine (*Instron 5585H*). Test temperatures were ambient, 150 °C, 250 °C and 350 °C. As reported by the authors, Young modulus E has been identified through the elastic recovery identified in the loading and unloading of the AlSi-PE specimen for each temperature in order to describe its evolution.

Furthermore, it must be emphasised that the specific heat capacity C_p of a material can also evolve with the increase in temperature, especially for metallic materials. Unfortunately, the values of AlSi-PE abradable specific heat capacity C_p in function of temperature were determined by our industrial partner and cannot be communicated. By considering the modeling approach in this study, an incremental calculation method was developed, taking into account temperature, Young modulus and specific heat capacity evolution of the sample in the optimization algorithm of the Johnson-Cook constitutive law. Therefore, this method correlates experimental data and modeling in an optimal manner. The description of this method is presented on Figure 3. Through this algorithm, the adiabatic heating of a 15 mm diameter and 7.5 mm thickness AlSi-PE specimen tested at 1200 s^{-1} using the SHPB setup was estimated. This particular characterization has been done for each tested temperature, ranging from ambient up to 360 °C. On Figure 4, results illustrate that the higher the initial specimen temperature, the less significant the adiabatic heating.

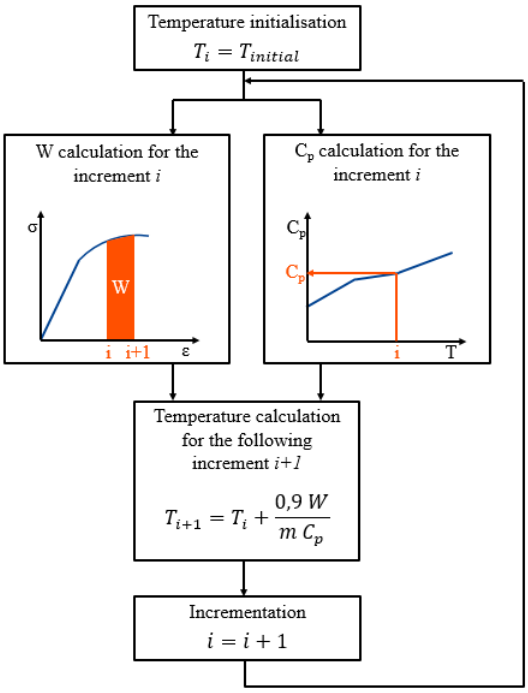

Figure 3: Diagram exhibiting the method of incremental calculation for adiabatic heating estimation

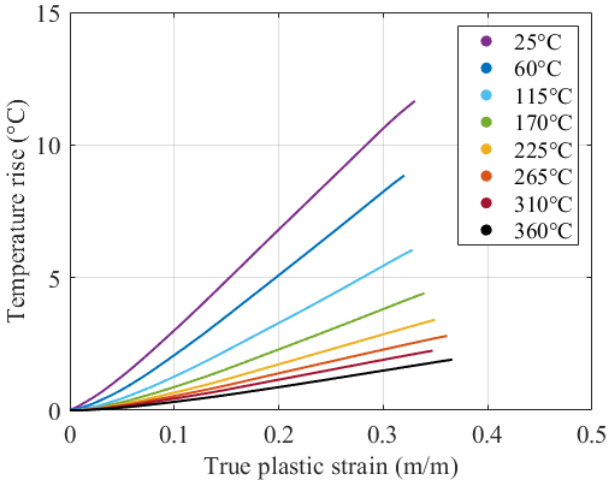

Figure 4: Estimated adiabatic heating for dynamic loading at a strain-rate of 1200 s^{-1} for an AlSi-PE specimen tested under a wide range of temperatures

Analyses of SHPB experimental data were carried out by taking into account stress equilibrium at the specimen interfaces during the first compressive loading [1]. Ravichandran and Subhash [29] established a criterion which determines, through a chosen threshold value, the portion of the test where the specimen reaches an equilibrium state. The chosen threshold value generally depends on the characterized material and can vary from 5% [29] to 30% [19, 30]. The nature of AlSi-PE abradable induces a relatively high threshold value due to its complex dynamical behavior. Skiba et al. [1] gave a much more detailed description of the dynamic tests analysis method. By considering this previous information, a threshold value of 20% was chosen. It is worth mentioning that this equilibrium criterion is highly sensitive to the initial filtering of the signals. Therefore, in this study, a 100 kHz low-pass filter has been applied for the whole set of dynamic tests. Figure 5 exhibits the evolution of the Ravichandran criterion for a strain-rate of 1200 s^{-1} at ambient temperature and 350 °C. Hence, with a threshold value of 20%, a section of the dynamic tests was not considered for the mechanical behavior characterization (dotted lines in Figures 5 and 6). Results indicated a shortening of the section at an equilibrium state with increasing temperatures. This study was carried out in each temperature test, with no unloading ever being used. Corresponding results are shown on Figure 6 through true stress-strain data, where only the equilibrium state (full lines) of the curves is considered in the following modeling study.

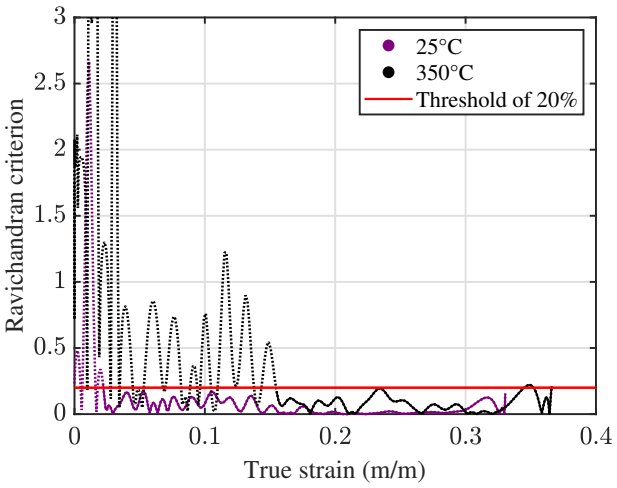

Figure 5: Ravichandran criterion expression with values $> 20\%$ (dotted lines) and $\leq 20\%$ (full lines) - AlSi-PE abradable coating at room temperature and 350 °C for a strain-rate of 1200 s^{-1}

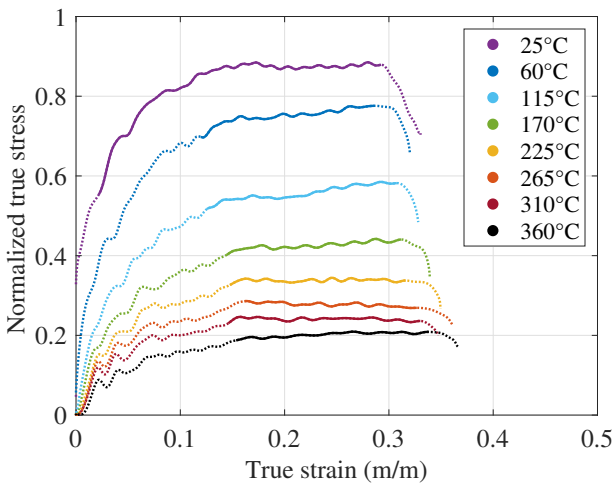

Figure 6: Compressive stress-strain curves of an AlSi-PE abradable from room temperature to 360 °C at 1200 s^{-1} - non-equilibrium state (dotted lines) and equilibrium state with a threshold value chosen at 20% (solid lines)

Figure 6 indicates a low elastic deformation for each temperature, followed by a significant plastic deformation section until fracture reaches its fracture point. Additionally, it highlights a strong temperature dependence of the AlSi-PE abradable mechanical behavior, and a reduced equilibrium state between 60 °C and 360 °C.

3.3. AlSi-PE abradable thermoviscoplastic behavior modeling

As described by Skiba et al. in a previous research work [1], AlSi-PE coating's behavior highlights a strong temperature dependence at 1200 s^{-1}. Furthermore, in another study Skiba et al. [2] put forward the same statement in quasi-static conditions, i.e. an explicit mechanical hardening with cyclic quasi-static tests and a strain-rate sensitivity between monotonous quasi-static and dynamic tests on AlSi-PE coating. Considering these experimental observations, the goal was to use a precise formalism of constitutive law that expresses the stated AlSi-PE thermomechanical behavior. Hence, by considering the specific nature of the tested coating material, particular attention was paid to existing constitutive laws for metallic materials. Therefore, the Johnson-Cook constitutive law formulation [31] seemed very suitable here to describe AlSi-PE thermoviscoplastic behavior. This constitutive law is typically applied for homogeneous metallic materials, which generally exhibit a mechanical hardening and are sensitive to strain-rate and temperature changes in compressive/tensile loading [31]. Figure 7 highlights this statement in an AlSi-PE framework for the three distinct parts of the JC constitutive law.

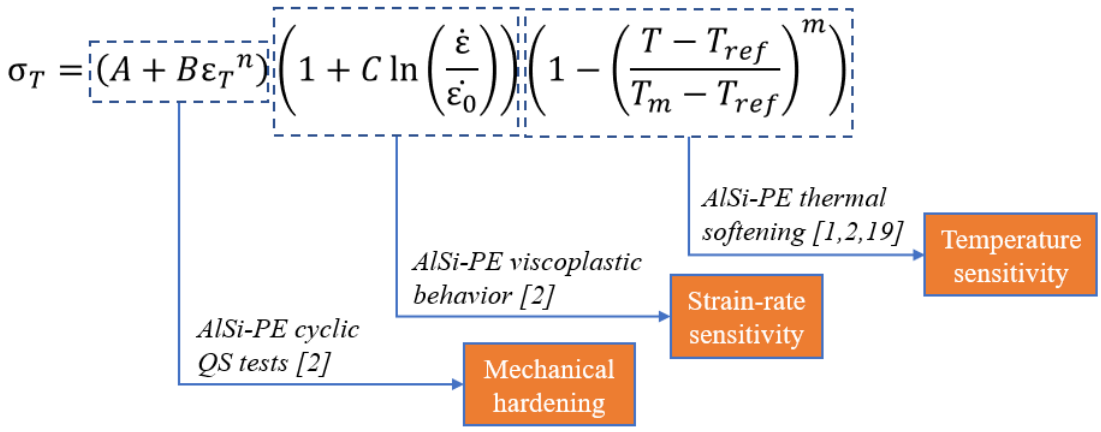

Figure 7: Diagram of the Johnson-Cook constitutive law structure in regard to an AlSi-PE coating framework

All the dynamic and quasi-static results of the AlSi-PE abradable material are presented in this section in correlation with a JC constitutive law considering the true strain ε_T and stress σ_T data. The expression of this phenomenological law can be seen in equation 6.

$$\sigma_T = (A + B\varepsilon_T{}^n)\left(1 + C\ln\left(\frac{\dot{\varepsilon}}{\dot{\varepsilon}_0}\right)\right)\left(1 - \left(\frac{T - T_{ref}}{T_t - T_{ref}}\right)^m\right) \tag{6}$$

This equation is based on JC law parameters A, B, C, n and m. A, B and n represent the mechanical hardening, C the strain-rate sensitivity and m the temperature sensitivity of the material. The melting temperature T_m, normally included in the JC formulation, is not suitable for AlSi-PE coating, considering its multi-phase nature. Thus, the original T_m parameter has been replaced by the T_t parameter, which describes the temperature at which the material deforms plastically without any stress being applied. Thus, T_t has been introduced in the JC formulation as a parameter to be determined from experimental data as well. $\dot{\varepsilon}_0$ is equal to 0.0017 s^{-1} corresponding to the strain-rate set for quasi-static experiments and T_{ref} is equal to 25 °C corresponding to the lowest temperature of the whole experimental campaign. Parameter T in equation 6, representing the temperature of the specimen during loading, includes the estimated adiabatic heating of the specimen for high strain-rates tests (Figure 4). Indeed the resulting rise in temperature may modify its mechanical response and has to be accounted for. All of these parameters were determined from experimental data using the *Global Search* Matlab® optimization function with *fmincon* solver based on the *interior-point* algorithm. Corresponding results are listed in Table 1. Figures 8 and 9 propose a comparison between experimental results and model identifications for a large range of temperatures at 0.0017 s^{-1} and 1200 s^{-1}. The same comparison has been made on Figure 10 at room temperature and at different strain-rates. Both quasi-static and dynamic results above 250 °C do not fit well with JC constitutive law, especially for the tests conducted at high temperatures and at 1200 s^{-1}.

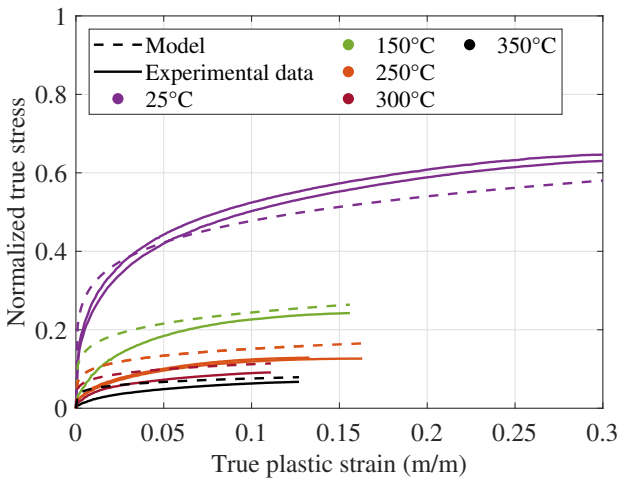

Figure 8: JC model - experimental results comparison of the quasi-static tests at 0.0017 s^{-1} for a wide range of temperatures

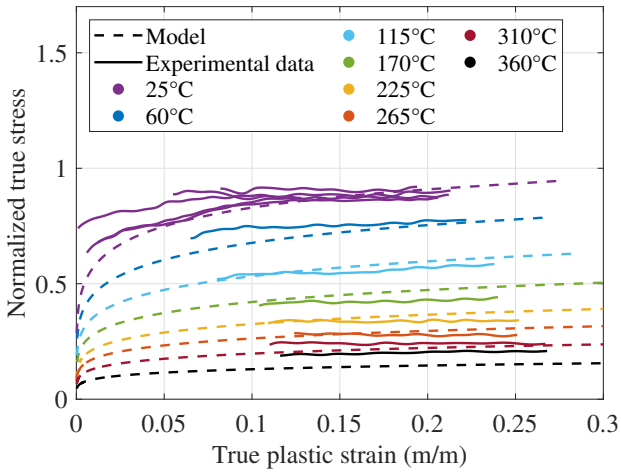

Figure 9: JC model - experimental results comparison of the dynamic tests at 1200 s^{-1} for a wide range of temperatures

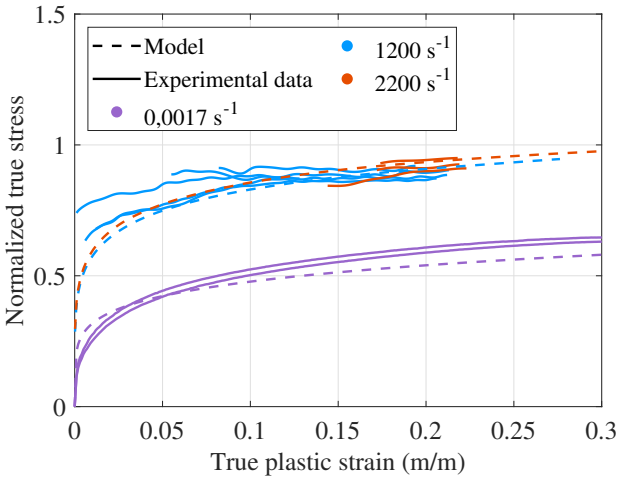

Figure 10: JC model - experimental results comparison of dynamic and quasi-static tests at ambient temperature

Normalized $\boldsymbol{A}$	Normalized $\boldsymbol{B}$	$\boldsymbol{n}$	$\boldsymbol{m}$	$\boldsymbol{C}$	T_t (°C)
6.66×10^{-7}	0.719	0.177	0.564	0.066	465.72

Table 1: Normalized Johnson-Cook parameters identification

Several factors could explain these discrepancies, such as masked reliances between the three main parts of the JC constitutive law previously mentioned. Temperature reliance with other parameters has mainly been studied since it has the strongest influence on the AlSi-PE mechanical response. Multiple modifications of the JC law have been tested, such as an exponential mechanical hardening, the effect of adiabatic heating on JC law at 1200 s^{-1}, which only exhibits a difference of the mechanical hardening at room temperature through

Figure 11, or the connection between temperature and strain-rate. Results have shown that the strain-rate sensitivity parameter C outweighs other potential reliance in regards with temperature dependency.

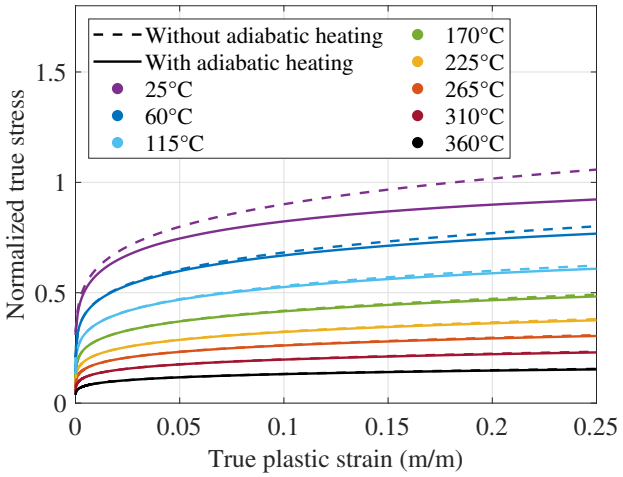

Figure 11: Effects of adiabatic heating on JC constitutive law application at 1200 s^{-1} for a wide range of temperatures

To take into account parameter C evolution through temperature changes, a new formulation has been proposed with a dependence of the strain-rate sensitivity parameter C upon the temperature T. As a first step, the main goal was to assimilate each dynamic temperature test with a corresponding quasi-static temperature test. Thus, five of the eight dynamic tests have been brought together with quasi-static tests in regard to the closest values of the following temperatures : RT, 150 °C, 250 °C, 300 °C and 350 °C. For instance, the dynamic test made at 265 °C has been coupled with the quasi-static test made at 250 °C. As a final step, the five quasi-static and dynamic tests have been correlated through the optimization algorithm to identify a corresponding value of the strain-rate sensitivity C parameter for each temperature. Results are exhibited in Figure 12. The relation describing the exponential dependence between parameter C and temperature can be seen in equation 7, whose formulation is explained by the exponential shape of the strain-rate sensitivity C parameter with increasing temperature (Figure 12). Finally, equation 8 depicts the integration of equation 7 into the initial version of the JC constitutive law, thus forming the original expression named AlSi-PE Constitutive Law (ASPECL), aiming to model the thermoviscoplastic behavior of AlSi-PE coating.

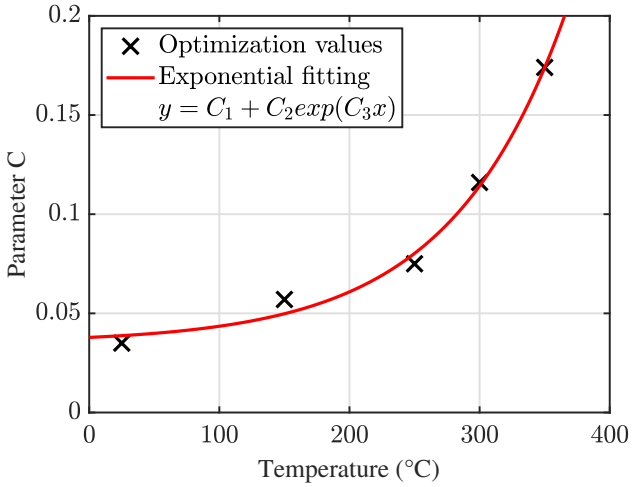

Figure 12: Evolution of the strain-rate sensitivity C parameter with respect to temperature

This formulation introduces three new parameters, C_1, C_2 and C_3, which have also been determined from experimental data. All the parameters are listed in Table 2. All the correlations between experimental results and model identifications are presented in Figures 13, 14 and 15.

$$C = (C_1 + C_2 \exp(C_3 T)) \tag{7}$$

$$\sigma_T = (A + B{\varepsilon_T}^n)\left(1 + (C_1 + C_2 \exp(C_3 T)) \ln\left(\frac{\dot{\varepsilon}}{\dot{\varepsilon}_0}\right)\right)\left(1 - \left(\frac{T - T_{ref}}{T_t - T_{ref}}\right)^m\right) \tag{8}$$

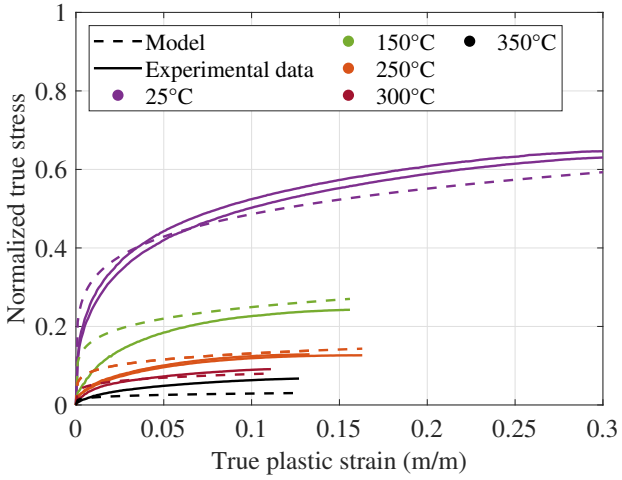

Figure 13: ASPECL modeling - experimental results comparison of the quasi-static tests at 0.0017 s^{-1} for a wide range of temperatures

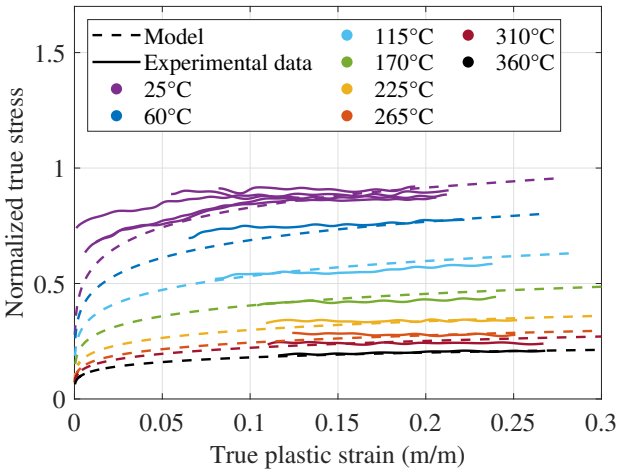

Figure 14: ASPECL modeling - experimental results comparison of the dynamic tests at 1200 s^{-1} for a wide range of temperatures

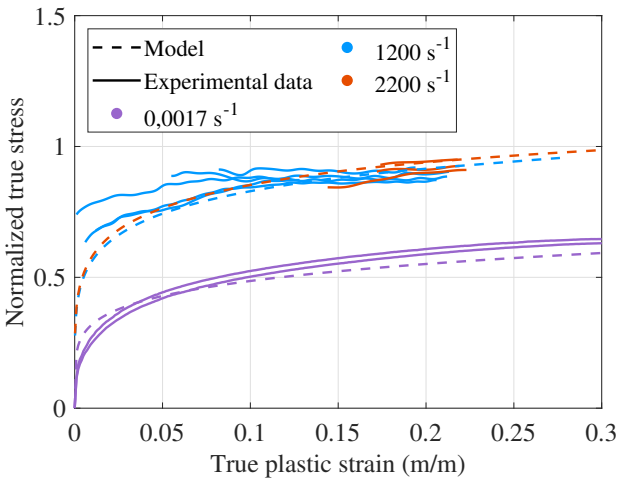

Figure 15: ASPECL modeling - experimental results comparison of dynamic and quasi-static tests at ambient temperature

Normalized $\boldsymbol{A}$	Normalized $\boldsymbol{B}$	$\boldsymbol{n}$	$\boldsymbol{m}$	C_1	C_2	C_3	T_t (°C)
0.0012	0.736	0.181	0.688	0.06	3.39×10^{-6}	0.033	380.47

Table 2: Normalized ASPECL parameters identification

Due to the correction of parameter C, Figures 13, 14 and 15 exhibit a better correlation between experimental results and the AlSi-PE constitutive law at high temperatures and strain-rate (1200 s^{-1}). These observations are supported by the expression of the approximation error between experimental and modeling data. This analysis has been made for both constitutive laws for tests conducted at 1200 s^{-1} for a wide range of temperatures. The mean approximation error, named $\overline{\delta}$ here, has been estimated through equation 9, where $\sigma(\varepsilon_p)^{exp}$ represents the stress/plastic strain evolution obtained by experimental means, $\sigma(\varepsilon_p)^{mod}$ the stress/plastic strain evolution described by constitutive laws and n the total number of data points. It must be noted that this calculation has only been done over the stress equilibrium state for dynamic testing data.

$$\overline{\delta} = \frac{1}{n}\sum_{i=1}^{n}\frac{\left|\sigma_i(\varepsilon_p)^{exp} - \sigma_i(\varepsilon_p)^{mod}\right|}{\left|\sigma_i(\varepsilon_p)^{exp}\right|} * 100 \tag{9}$$

The results can be seen on Figure 16. The mean approximation error remains below 10% for both modeling approaches at temperatures ranging from 25 °C up to 310 °C but increases greatly at 360 °C for the JC model. These observations highlight the relevance of the ASPECL formulation, especially at 360 °C where the error $\overline{\delta}$ is the lowest. Even though the results are not presented here, a similar study was performed for different strain-rates at ambient temperature. This study exhibited a low influence of the strain-rate on the accuracy of both modeling approaches with close error values below 10%. Thus, the addition of the exponential dependence between temperature and the strain-rate sensitivity parameter seems to be the most

appropriate to translate the thermomechanical behavior of AlSi-PE coating.

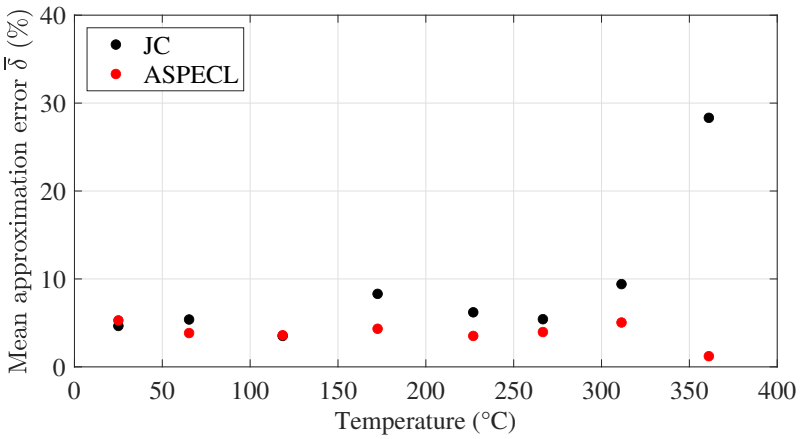

Figure 16: Evolution of the modeling/experimental data error for the classical JC formulation and ASPECL in function of temperature for tests conducted at a strain-rate of 1200 s^{-1} and for temperatures ranging from 25 °C up to 360 °C

3.4. Johnson-Cook damage initiation of the AlSi-PE abradable coating

In some numerical models, such as cutting or friction models, wear can be represented, as the interaction progresses, by successively disabling elements whose plastic strain exceeds a theoretical strain to failure. Through their thermomechanical friction model, Chassaing et al. [32] defined the strain to failure with a computational failure model based on the Johnson-Cook damage law [33]. By using this method, wear could be defined through blade/abradable coating interaction numerical models thanks to identification of the JC damage law parameters for abradable coatings. Since the modeling of the AlSi-PE thermomechanical behavior went further with the AlSi-PE constitutive law which adequately simulates its response, a study regarding the prediction of strains to failure based on experimental data has been led on AlSi-PE coating. Therefore, the JC damage law has been coupled with the original formulation presented previously. The damage initiation strain, or strain to failure, defined by ε_p^f in equation 10, represents the plastic strain value from which failure of the specimen theoretically begins. The formulation of this law in equation 10 is based on damage Johnson-Cook parameters $D_1 \sim D_5$, transition temperature T_t, and constants $\dot{\varepsilon_0}$ and T_0. $D_1 \sim D_5$ are parameters obtained from experimental data on cylindrical specimens at different strain-rates and temperatures.

$$\varepsilon_p^f = (D_1 + D_2 \exp(\sigma^* D_3)) \left(1 + D_4 \ln\left(\frac{\dot{\varepsilon}}{\dot{\varepsilon}_0}\right)\right) \left(1 + D_5 \left(\frac{T - T_{ref}}{T_t - T_{ref}}\right)\right) \tag{10}$$

Besides, in order to account for stress state (such as stress tri-axiality), a dimensionless hydrostatic pressure coefficient σ^* has been used, which can be calculated with the following expressions in equations 11, 12 and 13, where σ_m and σ_{vm} are the averages of the three principal stresses and the Von Mises equivalent

stress respectively.

$$\sigma^* = \frac{\sigma_m}{\sigma_{vm}} \tag{11}$$

$$\sigma_m = \frac{1}{3}\, tr([\sigma]) \tag{12}$$

$$\sigma_{vm} = \sqrt{\frac{1}{2}((\sigma_{xx} - \sigma_{yy})^2 + (\sigma_{yy} - \sigma_{zz})^2 + (\sigma_{zz} - \sigma_{xx})^2)} \tag{13}$$

Only the principal stress σ_{yy} is considered here, due to the fact that an uni-axial compression hypothesis has been imposed for SHPB and QS tests. Thus, all the calculations of the damage initiation law have been done with $\sigma^* = 1/3$. This assumption can be supported by the work of Bai and Wierzbicki [34]. In addition, tests conducted at 2200 s^{-1} were only submitted to ambient temperature, and by considering that tests at 1200 s^{-1} did not lead to failure at any given temperature, the relevance of the damage initiation law application for dynamic tests can be questioned. Based on this statement, only quasi-static tests have been taken into account, setting aside strain-rate sensitivity in this particular study. The corresponding formulation of the law is presented equation 14. As for the previous law, temperature of reference T_{ref} was set to 25 °C.

$$\varepsilon_p^f = \left(D_1 + D_2 \exp\left(-\frac{1}{3}D_3\right)\right)\left(1 + D_5\left(\frac{T - T_{ref}}{T_t - T_{ref}}\right)\right) \tag{14}$$

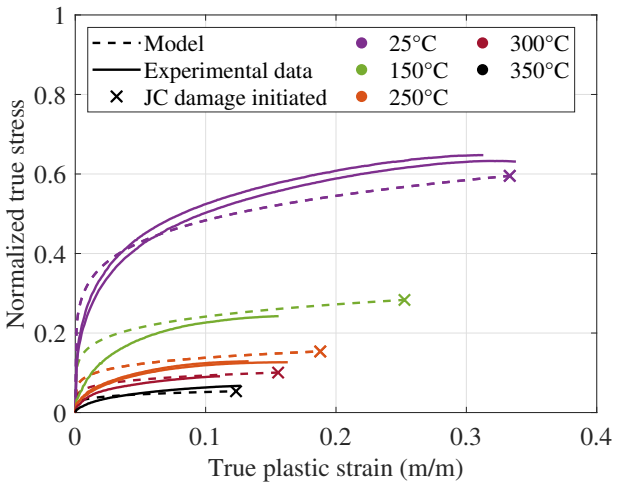

Figure 17: ASPECL modeling - experimental results comparison coupled with JC damage initiation criterion of the quasi-static tests at 0.0017 s^{-1} for a wide range of temperatures

D_1	D_2	D_3	D_5	T_t (°C)
1.046	−2.094	3.234	−0.732	402.6

Table 3: JC damage law parameters identification

Corresponding results of the AlSi-PE constitutive law coupled with the JC strain to failure (represented by a cross) at a low strain-rate for a wide range of temperatures are exhibited on Figure 17. A satisfactory correlation can be observed between the greatest plastic strain of experimental data and the theoretical strain to failure at room temperature and 350 °C. Although only phenomenological modeling laws are presented in this research work, JC strains to failure at 150 °C, 250 °C and 300 °C do not seem to adequately express the macroscopic behavior of AlSi-PE coating. In order to obtain an optimal correlation, a new formulation of the JC damage initiation law has been proposed in equation 15. This new approach takes into account temperature sensitivity through parameter m (in red), which is included such as the temperature sensitivity parameter in a classical Johnson-Cook constitutive law for matching the power-like shape of quasi-static tests. All the parameters corresponding to this new expression are listed on Table 4.

$$\varepsilon_p^f = \left(D_1 + D_2 \exp\left(-\frac{1}{3}D_3\right)\right)\left(1 + D_5\left(\frac{T - T_{ref}}{T_t - T_{ref}}\right)^{m}\right) \tag{15}$$

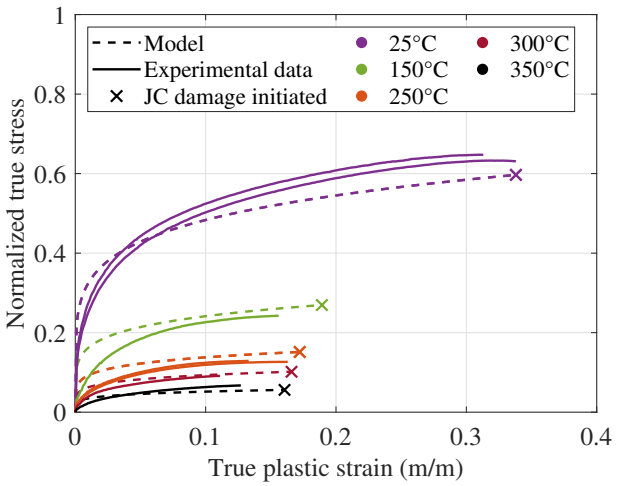

Figure 18: ASPECL modeling - experimental results comparison coupled with modified JC damage initiation criterion of the quasi-static tests at 0.0017 s^{-1} for a wide range of temperatures

D_1	D_2	D_3	D_5	$\boldsymbol{m}$	T_t (°C)
0.683	−1.309	4.006	−0.539	0.185	400

Table 4: Modified Johnson-Cook damage law parameters identification

As Figure 18 shows, this new formulation is in a better agreement with experimental data at 0.0017 s^{-1} for the large range of temperatures explored, especially at room temperature, 150 °C and 250 °C. Thereby, this modified damage law is able to accurately predict failure of porous and heterogeneous AlSi-PE specimens with a temperature increase in quasi-static conditions.

4. Conclusions

The main objective of this study was to put forward a constitutive law able to forecast the thermomechanical behavior of the AlSi-PE abradable coating as accurately as possible. By coupling a high speed camera with a dynamic SHPB test on a speckle pattern specimen of AlSi-PE abradable coating, hypotheses have been verified in order to express quasi-static and dynamic experimental data through true values, and consequently identify the parameters of a standard JC constitutive law. Although correlation results between experimental data and the JC law were quite satisfactory, an original constitutive law has been proposed, taking into account an exponential dependence between the strain-rate sensitivity parameter and temperature, to reach an optimal correlation at high temperatures for a strain-rate of $1200\ s^{-1}$. Finally, a standard and a modified Johnson-Cook damage laws have been introduced into the AlSi-PE behavior modeling for predicting damage initiation in quasi-static conditions. Test results demonstrated that experimental tests conducted at $0.0017\ s^{-1}$ were in reasonable agreement with this damage criterion.

Declaration of competing interest

The authors declare that they have no known competing financial interests or personal relationships that could have appeared to influence the work reported in this paper.

Acknowledgments

We gratefully acknowledge S. Skiba for his work that partially contributed to experimental data acquisition and *Safran Aircraft Engines*, which provided the abradable coating necessary for this study.

Data availability

The raw/processed data required to reproduce these findings cannot be shared at this time due to legal or ethical reasons.

References

[1] S. Skiba, L. Faure, S. Philippon, J. Papasidero, Experimental Investigation of the Mechanical Behavior of an AlSi-PE Abradable Coating at High Strain Rates for a Large Range of Temperatures, J. dynamic behavior mater. (2020).

[2] S. Skiba, B. Chevrier, L. Faure, S. Philippon, Thermoelastoviscoplastic Bilinear Compressive Constitutive Law of an AlSi-PE Abradable Material Based on Experimental Investigations, J. dynamic behavior mater. (2021).

[3] M. Bounazef, S. Guessasma, E. A. A. Bedia, Blade protection and efficiency preservation of a turbine by a sacrificial material coating, Advanced Powder Technology 18 (2007) 123–133.

[4] M. O. Borel, A. R. Nicoll, H. W. S. Pfer, R. K. Schmid, The wear mechanisms occurring in abradable seals of gas turbines 40 (1989) 117–126.

[5] C. Padova, J. Barton, M. Dunn, S. Manwaring, G. Young, M. Adams, M. Adams, Development of an Experimental Capability to Produce Controlled Blade Tip / Shroud Rubs at Engine Speed (2017) 0–10.

[6] N. Fois, J. Stringer, M. B. Marshall, Adhesive transfer in aero-engine abradable linings contact, Wear 304 (2013) 202–210.

[7] J. Stringer, M. B. Marshall, High speed wear testing of an abradable coating, Wear 294-295 (2012) 257–263.

[8] C. Delebarre, V. Wagner, J. Y. Paris, G. Dessein, J. Denape, J. Gurt-Santanach, An experimental study of the high speed interaction between a labyrinth seal and an abradable coating in a turbo-engine application, Wear 316 (2014) 109–118.

[9] M. Watson, M. Marshall, Wear mechanisms at the blade tip seal interface, Wear 404-405 (2018) 176–193.

[10] W. Xue, S. Gao, D. Duan, J. Zhang, Y. Liu, S. Li, Effects of blade material characteristics on the high-speed rubbing behavior between Al-hBN abradable seal coatings and blades, Wear 410-411 (2018) 25–33.

[11] P. Schmiechen, Travelling Wave Speed Coincidence, Medicine (1997).

[12] A. Millecamps, J.-F. Brunel, P. Dufrenoy, F. Garcin, M. Nucci, Etude thermomécanique du contact aube-carter d'un turboréacteur et conséquence sur son excitation dynamique, 19ème Congrès Français de Mécanique (2009) 24–28.

[13] R. Schmid, New high temperature abradables for gas turbines, Ph.D. thesis, Swiss Federal Institute of Technology Zurich, 1997.

[14] B. Martinet, A. Cappella, S. Philippon, C. Montebello, Effect of temperature on wear mechanisms of an aluminium - Based abradable coating for aircraft engines after a dynamic interaction with a Ti6al4v blade, Wear 446-447 (2020) 203202.

[15] A. Millecamps, A. Batailly, M. Legrand, F. Garcin, Snecma ' s Viewpoint on the Numerical and Experimental Simulation of Blade-Tip / Casing Unilateral Contacts To cite this version : HAL Id : hal-01223582 Snecma ' s viewpoint on the numerical and experimental simulation of blade-tip / casing unilateral contacts (2015).

[16] G. Jacquet-richardet, M. Torkhani, P. Cartraud, F. Thouverez, T. Nouri-baranger, M. Herran, C. Gibert, S. Baguet, P. Almeida, L. Peletan, Rotor to stator contacts in turbomachines . Review and application To cite this version : HAL Id : hal-00934050 Rotor to stator contacts in turbomachines . Review and application HAL Id : hal-01381113 (2016).

[17] M. Legrand, A. Batailly, C. Pierre, Numerical investigation of abradable coating removal in aircraft engines through plastic constitutive law, Journal of Computational and Nonlinear Dynamics 7 (2012).

[18] A. Batailly, M. Cuny, M. Legrand, S. Philippon, Numerical-experimental confrontation in the simulation of tool / abradable material interaction To cite this version : HAL Id : hal-00826981 (2014) 0–19.

[19] A. Pellegrino, P. M. M. Jesus, K. Dragnevski, G. Zumpano, N. Petrinic, Temperature and strain rate dependent mechanical response of METCO 601 aluminium-polyester abradable seal coating, EPJ Web of Conferences 183 (2018) 1–6.

[20] A. Batailly, M. Legrand, C. Pierre, Full Three-Dimensional Rotor / Stator Interaction Simulations in Aircraft Engines With Time-Dependent Angular Speed To cite this version : HAL Id : hal-01388425 time-dependent angular speed Simulations 3D d ' interactions rotor / stator dans des moteurs d (2019) 0–15.

[21] T. Nicholas, Dynamic Tensile Testing of Structural Materials Using a Split Hopkinson Bar Apparatus, Technical Report, 1980.

[22] J. L. Lewis, J. D. Campbell, The development and use of a torsional Hopkinson-bar apparatus, Experimental Mechanics 12 (1972) 520–524.

[23] R. J. Christensen, S. R. Swanson, W. S. Brown, Split-hopkinson-bar tests on rock under confining pressure - Description of apparatus and test results is given. Attention is given to complete measurement of principal strain and resolution of initial stress-strain data, Experimental Mechanics 12 (1972) 508–513.

[24] K. T. Ramesh, S. Narasimhan, Finite deformations and the dynamic measurement of radial strains in compression Kolsky bar experiments, International Journal of Solids and Structures 33 (1996) 3723–3738.

[25] J. Blaber, B. Adair, A. Antoniou, Ncorr: Open-Source 2D Digital Image Correlation Matlab Software, Experimental Mechanics 55 (2015) 1105–1122.

[26] G. I. Taylor, H. Quinney, The Latent Energy Remaining in a Metal after Cold Working, Proceedings of the Royal Society A: Mathematical, Physical and Engineering Sciences 143 (1934) 307–326.

[27] D. Rittel, L. H. Zhang, S. Osovski, The dependence of the Taylor–Quinney coefficient on the dynamic loading mode, Journal of the Mechanics and Physics of Solids 107 (2017) 96–114.

[28] R. B. McLellan, T. Ishikawa, The elastic properties of aluminum at high temperatures, Journal of Physics and Chemistry of Solids 48 (1987) 603–606.

[29] G. Ravichandran, G. Subhash, Critical Appraisal of Limiting Strain Rates for Compression Testing of Ceramics in a Split Hopkinson Pressure Bar, Journal of the American Ceramic Society 77 (1994) 263–267.

[30] B. Song, W. Chen, Split Hopkinson pressure bar techniques for characterizing soft materials, Latin American Journal of Solids and Structures 2 (2005) 113–152.

[31] G. R. Johnson, W. H. Cook, A Computational Constitutive Model and Data for Metals Subjected to Large Strain, High Strain Rates and High Pressures, the Seventh International Symposium on Ballistics (1983) 541–547.

[32] G. Chassaing, A. Pougis, S. Philippon, P. Lipinski, J. Meriaux, L. Faure, Initiation of Adhesive Wear During Frictional Interaction at Very High Velocity for a Ti6Al4V Tribopair, Proceedings of the 13th World Conference on Titanium (2016) 1637–1642.

[33] G. R. Johnson, W. H. Cook, Fracture characteristics of three metals subjected to various strains, strain rates, temperatures and pressures, Engineering Fracture Mechanics 21 (1985) 31–48.

[34] Y. Bai, T. Wierzbicki, A new model of metal plasticity and fracture with pressure and Lode dependence, International Journal of Plasticity 24 (2008) 1071–1096.

Identification of constitutive laws' parameters by means of experimental tests on AlSi-PE abradable coating

B. Chevrier, J. Vincent, L. Faure, S. Philippon

Dynamic conditions : SHPB tests conducted at $1200\ s^{-1}$ *and* $2200\ s^{-1}$

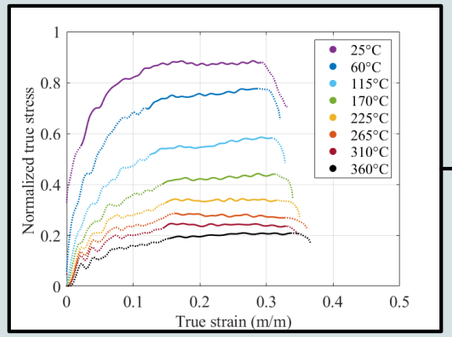

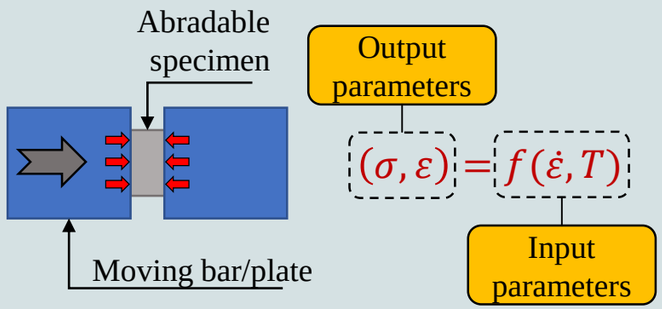

Quasi-static conditions : QS compression tests conducted at $0.0017\ s^{-1}$

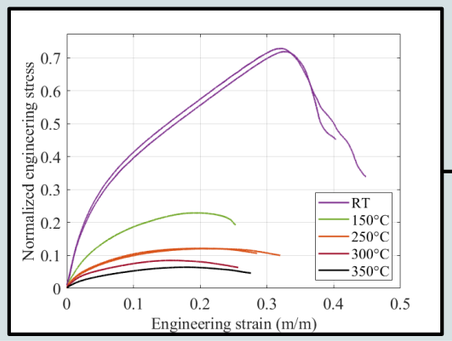

Constitutive law

$$\sigma_T = (A + B\varepsilon_T{}^n)\left(1 + (C_1 + C_2 \exp(C_3 T)) \ln\left(\frac{\dot{\varepsilon}}{\dot{\varepsilon}_0}\right)\right)\left(1 - \left(\frac{T - T_{ref}}{T_t - T_{ref}}\right)^m\right)$$

AlSi-PE cyclic QS tests [2] → Mechanical hardening

AlSi-PE viscoplastic behavior [2] → Strain-rate sensitivity

AlSi-PE thermal softening [1,2,19] → Temperature sensitivity

Damage law

$$\varepsilon_p^f = \left(D_1 + D_2 \exp\left(-\frac{1}{3} D_3\right)\right)\left(1 + D_5 \left(\frac{T - T_{ref}}{T_t - T_{ref}}\right)^m\right)$$

Modeling / dynamic experimental data correlation

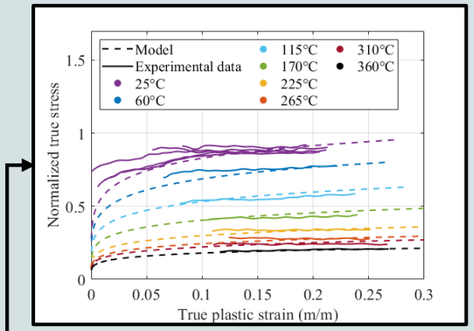

Modeling / QS experimental data correlation

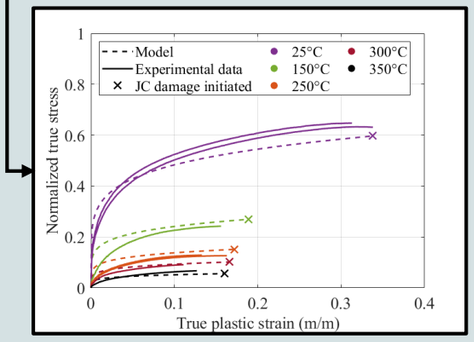

LEM3 LABORATOIRE D'ÉTUDE DES MICROSTRUCTURES ET DE MÉCANIQUE DES MATÉRIAUX
ENIM École nationale d'Ingénieurs de Metz
UNIVERSITÉ DE LORRAINE
SAFRAN AIRCRAFT ENGINES